Bull. Chem. Soc. Ethiop. **2025**, 39(2), 313-326.
DOI: https://dx.doi.org/10.4314/bcse.v39i2.10

ISSN 1011-3924
Printed in Ethiopia
Online ISSN 1726-801X

SYNTHESIS, CHARACTERIZATION, AND BIOLOGICAL EVALUATION OF ZINC(II) COMPLEXES WITH BENZOHYDRAZIDE DERIVATIVE AND PHOSPHINE LIGANDS

Nazk M. Aziz[1*] and Ahmad A. Irzoqi[2]

[1]Department of Chemistry, College of Science, University of Suliamani, KRG-Iraq

[2]Department of Chemistry, College of Education for Pure Science, University of Tikrit, Tikrit, Iraq

(Received August 22, 2024; Revised October 28, 2024; Accepted October 29, 2024)

Abstract. New zinc(II) complexes of the mixed ligands were synthesized using a benzohydrazide derivative (L), yielded from reaction of benzohydrazide and isatin, in combination with (Phen) and various phosphine co-ligands, including 1,10-phenanthroline (Phen), 1,2-bis(diphenylphosphino)ethane(dppe), 1,2-bis(diphenylphosphino) propane (dppp), and triphenylphosphine (PPh_3). Characterization methods included molar conductivity, atomic absorption, FTIR, and ^{1}H, $^{13}C\{^{1}H\}$,$^{31}P\{^{1}H\}$-NMR spectroscopy, confirming tetrahedral geometry around zinc(II) with the ligand N'-(2-oxoindolin-3-ylidene) benzohydrazide (L) acting as a bidentate chelating ligand. The thermogravimetric (TG) analysis of the papered complexes $[Zn(L)(Phen)]Cl_2$, $[Zn(L)(PPh_3)]Cl_2$, and $[Zn(L)(dppp)]Cl_2$ showed that each of them has been decomposed in three stages. The in vitro biological activities were evaluated against four types of bacteria, *Staphylococcus aureus*, *Streptococcus faecalis*, *Pseudomonas aeruginosa*, and *Escherichia coli*, along with cancer human liver (Hep-G2) cell lines, revealing that the complexes exhibited significant cytotoxicity. Notably, the $[Zn(L)(Phen)]Cl_2$ complex showed the strongest inhibitory effect on human liver (Hep-G2) cells, with an IC_{50} of 31.12 ± 1.57 μM. Antibacterial tests indicated that $[Zn(L)(Phen)]Cl_2$ and $[Zn(L)(dppp)]Cl_2$ complexes effectively inhibited *Streptococcus faecalis*, and $[Zn(L)(Phen)]Cl_2$ also had limited efficacy against Gram-negative bacteria. Structure-activity relationship studies highlighted that the choice of phosphine ligand significantly influences the biological properties of these zinc(II) complexes.

KEY WORDS: Antibacterial, Anticancer, Benzohydrazide derivative, Mixed ligands complexes, Phosphines, Spectroscopy

INTRODUCTION

New zinc(II) complexes featuring isatin Schiff bases or *N′*-(2-oxoindolin-3-ylidene) benzohydrazide (L) and phosphine ligands have received significant research interest due to their unique structural and functional properties, which offer diverse coordination geometries and potential applications in medicinal chemistry and industry.

Isatin, an indole derivative, is a naturally occurring compound found in plants of the isatis genus [1, 2]. Isatin possesses several unique properties, including electrophilic behavior, and serves as a key structural unit in the synthesis of various organic and heterocyclic compounds. Its derivatives exhibit a wide range of biological and pharmacological activities, including antibacterial, anticancer, and anti-HIV properties [3]. These derivatives are utilized in organic synthesis, the production of dyes, and even as precursors in the synthesis of illicit drugs [4, 5]. As a versatile ligand, isatin can be employed alone or in combination with other ligands, such as Schiff bases, formed by its reaction with amino groups [6]. This ability to form coordination complexes has been extensively studied, particularly involving transition metals. Research shows that complexes derived from isatin Schiff bases exhibit promising medical and biological applications [7, 8]. Numerous studies have demonstrated the diverse activities of isatin Schiff base derivatives, including antibacterial, antifungal, antiviral, anticancer, anti-inflammatory, and

*Corresponding authors. E-mail: nazk.aziz@univsul.edu.iq

anticonvulsant effects [9]. Recent investigations into the biological activity of isatin derivatives have led to the synthesis of various complexes. For instance, compounds like isatin-3-thiosemicarbazone have shown significant anti-inflammatory and antifungal activity [10-13]. Other studies have highlighted the potential of isatin-based complexes as inhibitors of the HDAC enzyme, show casing their anticancer properties [7, 8]. Furthermore, isatin derivatives have been synthesized in combination with different metal ions, resulting in complexes that exhibit notable biological activity [14-16]. Alongside the unique roles of isatin derivative complexes, diphosphines and phosphine metal complexes have received considerable attention in recent years for their antitumor effects, both in vitro and in vivo [17, 18]. This study seeks to explore the synthesis, characterization, and biological activities of novel zinc(II) complexes that incorporate isatin Schiff base and phosphine ligands, highlighting their potential in therapeutic applications.

EXPERIMENTAL

Materials

Various chemicals and reagents were purchased from different suppliers, including zinc(II) chloride ($ZnCl_2$), $C_{12}H_8N_2$ (Phen), $C_{26}H_{24}P_2$ (dppe), $C_{27}H_{26}P_2$ (dppp), and $P(C_6H_5)_3$ (PPh_3). Additionally, methyl benzoate, hydrazine, isatin, glacial acetic acid, ethanol, chloroform, DMSO, and diethyl ether were sourced from Fluka, BDH, Macklin, and Scharlau. Nuclear magnetic resonance (NMR) spectroscopy (^1H, $^{13}C\{^1H\}$, and $^{31}P\{^1H\}$) was performed using a Bruker instrument in the range (400 MHz, DMSO-d_6) at the University of Tehran, College of Science.

Preparation of the ligand N'-(2-oxoindolin-3-ylidene) benzohydrazide (L) [19, 20]

To prepare the ligand (L), the following two steps are implemented:

a. Step one. (1.412 g, 44.000 mmol) of hydrazine was directly added to (6.000 g, 44.000 mmol) of methyl benzoate, and the mixture was refluxed for three hours. The reaction was monitored with TLC. The crude product left to cool, orange precipitate obtained then filtered (the m.p 115 ^oC, 4.8 g, 80% yield).

b. Step two. A solution of benzohydrazide (2.776 g, 20.39 mmol) in (10 mL) of absolute ethanol was added to a suspension of isatin (3.000 g, 20.39 mmol) in (10 mL) of absolute ethanol, with the addition of a few drops of glacial acetic acid. The mixture was then heated under reflux. After 15 min, the color of the mixture changed from orange to yellow, and it was left under reflux for three hours, the reaction was monitored with TLC until completion. The product was then filtered, washed with cold ethanol, and dried in a vacuum oven (287-288 °C, 4.6 g, 85% yield). As shown in Scheme 1 step a (1) and step b (2)).

Synthesis of the zinc(II) complexes

a. Synthesis of the complex [Zn(L)(Phen)]Cl_2 ***1***

A hot solution of $ZnCl_2$(0.073 g, 0.542 mmol) in 10 mL of ethanol was added to a hot solution of the ligand (L) (0.144 g, 0.542 mmol) in 10 mL of absolute ethanol. The mixture was stirred for 15 minutes, and then Phen (0.107 g, 0.542 mmol) was added. The final mixture was heated under reflux for 3 hours, during which an orange precipitate formed. The precipitate was filtered, washed with cold ethanol, and then dried under vacuum. Orange solid, 95%, m.p.: 265-267 °C, IRν_{max} (cm^{-1}): 3201, 3166, 3056, 1695, 1676, 1531, 1515, 1429, 1344, 1269, 1149, 1097, 918, 842, 721, 686, 563. ^1H NMR (400 MHz, DMSO-d_6) δ (ppm): s, 13.94,1H,NH; s, 11.37, 1H, NH; d, 9.17, $^3J_{H-H}$ = 9.39 Hz , 2H, H1Phen; d, 8.78, $^3J_{H-H}$ = 9.39 Hz, 2H, H3Phen; s, 8.19, 2H, H4Phen; m, 8.08-

8.05, 4H, H_2Phen + H_e; d, 7.88, $^3J_{H\text{-}H}$ = 7.45 Hz, 1H, H_a; t, 7.60, $^3J_{H\text{-}H}$ = 7.49 Hz, 3H, H_f + H_g; t, 7.39, $^3J_{H\text{-}H}$ = 7.05 Hz, 1H, H_c; t, 7.11, $^3J_{H\text{-}H}$ = 7.68 Hz, 1H, H_b; d, 6.95, $^3J_{H\text{-}H}$ = 7.89 Hz, 1H, H_d. Λ_o (Ω^{-1}.cm^2.mol^{-1}) = 77.3, Zn% theoretical (practical) = 11.24 (11.09).

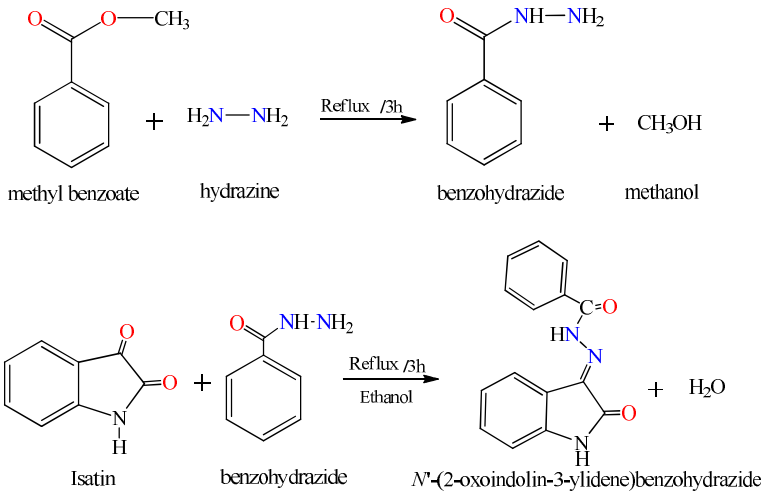

Scheme 1. Synthesis of the ligand *N*′-(2-oxoindolin-3-ylidene) benzohydrazide (L).

b. Synthesis of the complex [Zn(L)(PPh$_3$)Cl]Cl ***2***

A hot solution of $ZnCl_2$ (0.073 g, 0.542 mmol) in 10 mL of ethanol was added to a hot solution of (PPh_3) (0.142 g, 0.542 mmol) in 5 mL of absolute ethanol, and the mixture was heated under reflux. After one hour, a hot solution of the ligand (L) (0.144 g, 0.542 mmol) in 10 mL of absolute ethanol was added to the mixture. The final mixture was heated under reflux for 3 hours, during which a pale yellow precipitate formed. The precipitate was filtered, washed with cold ethanol, and then dried under vacuum. Pale yellow solid, 78%, m.p. 255-257 °C, IRν_{max} (cm^{-1}): 3193, 3172, 3056, 1695, 1677, 1620, 1533, 1434, 1269, 1149, 1000, 916, 750, 689, 501, 389. ^{1}H NMR (400 MHz, DMSO-d_6) δ (ppm): s, 13.97, 1H, NH; s, 11.41, 1H, NH; d, 7.92, $^3J_{H\text{-}H}$ = 6.94 Hz, 2H, He m, 7.72-7.59, 18H pph$_3$ + H_a + 2H_f ; t, 7.41, $^3J_{H\text{-}H}$ = 7.74 Hz, 1H, H_c; t, 7.13, $^3J_{H\text{-}H}$ = 7.54 Hz, 1H, H_b ; d, 6.98, $^3J_{H\text{-}H}$ = 7.80 Hz, 1H, H_d , ^{31}P{^{1}H}–NMR δ (ppm): δ = 32.61. Λ_o (Ω^{-1}.cm^2.mol^{-1}) = 32.7, Zn% theoretical (practical) =10.32 (10.14).

c. Synthesis of the complex [Zn(L)(PPh$_3$)$_2$]Cl$_2$ ***3***

A solution of $ZnCl_2$ (0.073 g, 0.542 mmol) in 10 mL of ethanol was added to a solution of the ligand (L) (0.1442 g, 0.542 mmol) in 10 mL of absolute ethanol, with stirring and heating. The mixture was then heated under reflux. After 1 hour, PPh_3 (0.482 g, 1.084 mmol) was added to the mixture, and the final mixture was heated under reflux for 3 hours. During this time, a dark yellow precipitate formed. The precipitate was filtered, washed with cold ethanol, and then dried under vacuum. Yellow solid, 80 %, m.p. 243-245 °C, IRν_{max} (cm^{-1}): 3195, 3170, 3070, 1695, 1676, 1533, 1481, 1431, 1344, 1269, 1149, 1095, 918, 752, 690, 503, 391. ^{1}H NMR (400 MHz, DMSO-d_6) δ (ppm): s, 13.93, 1H, NH; s, 11.37, 1H, NH; d, 7.89, $^3J_{H\text{-}H}$ = 7.21 Hz, 2H, H_e; d, 7.67, $^3J_{H\text{-}H}$ = 6.98 Hz, 1H, H_a m, 7.65-7.40, 33H 2, PPh_3 + 2H_f ; t, 7.39, $^3J_{H\text{-}H}$ = 7.82 Hz, 1H, H_c; t, 7.11, $^3J_{H\text{-}H}$ = 7.26 Hz, 1H, H_b ; d, 6.95, $^3J_{H\text{-}H}$ = 7.40 Hz, 1H, H_d , ^{31}P{^{1}H}–NMR δ (ppm): δ = 25.69. Λ_o (Ω^{-1}.cm^2. mol^{-1}) = 76.6, Zn% theoretical (practical) = 7.05 (7.20).

d. Synthesis of the complex [Zn(L)(dppe)]Cl_2 ***4***

A hot solution of $ZnCl_2$(0.073 g, 0.542 mmol) in 10 mL of ethanol was added to a hot solution of the ligand (L) (0.1442 g, 0.542 mmol) in 10 mL of absolute ethanol. The mixture was then heated under reflux for 1 hour. After 1 hour, a hot solution of dppe (0.299 g, 0.542 mmol) was added to the reaction mixture, and the final mixture was heated under reflux for 3 hours. During this time, a pale orange precipitate formed. The precipitate was filtered, washed with cold ethanol, and then dried under vacuum. Pale pink solid, 72 %, m.p.: 283-286 °C, IRν_{max} (cm^{-1}): 3243, 3056, 1687, 1623, 1537, 1469, 1429, 1269, 1151, 1099, 811, 750, 690, 528, 484. ^{1}H NMR (400 MHz, DMSO-d_6) δ (ppm): s, 13.96, 1H, NH; s, 11.41, 1H, NH; d, 7.93, $^3J_{H-H}$ = 6.89 Hz, 2H, H_e; d, 7.71, $^3J_{H-H}$ = 7.15 Hz, 1H, H_a, m, 7.67-7.54, 23H, dppe +2H_f ; t, 7.42 $^3J_{H-H}$ = 7.70 Hz 1H, H_c; t, 7.14, $^3J_{H-H}$ = 7.60 Hz, 1H, H_b ; d, 6.99, $^3J_{H-H}$ = 7.40 Hz, 1H, H_d; s, 2.85, 4H, 2CH_2, dppe, $^{31}P\{^1H\}$–NMR δ (ppm): δ = 29.97. Λ_o ($\Omega^{-1}.cm^2.mol^{-1}$) = 85.4, Zn% theoretical (practical) = 8.17 (7.99).

e. The synthesis of the [Zn(L)(dppp)]Cl_2 ***5***

The complex follows the same procedure, just substituting dppe (1,2-bis(diphenylphosphino)ethane) for the dppp (1,3-bis(diphenylphosphino)propane) ligand. The following (Scheme 2) shows the route of synthesized of Zn(II) complexes. Pale orange solid, 85 %, m.p. 249-251 °C, IRν_{max} (cm^{-1}): 3195, 3055, 1687, 1616, 1529, 1431, 1265, 1147, 1099, 933, 808, 746, 686, 505. ^{1}H NMR (400 MHz, DMSO-d_6) δ (ppm): s, 13.97, 1H, NH; s, 11.48 1H, NH; d, 7.93, $^3J_{H-H}$ = 6.81 Hz, 2H, He; m, 7.62-7.40; m, 7.86-7.80, 21H dppp + H_c ; d, 7.71, $^3J_{H-H}$ = 7.10 Hz, 1H, H_a; t, 7.64, $^3J_{H-H}$ = 7.20 Hz, 2H, H_f; t, 7.14, $^3J_{H-H}$ = 7.60 Hz, 1H, H_b; d, 7.00, $^3J_{H-H}$ = 7.80 Hz, 1H, H_d; t, 2.73, 4H, 2CH_2; m, 1.73, 2H, CH_2 dppp $^{31}P\{^1H\}$–NMR δ (ppm): δ = 57.70. Λ_o (Ω^{-1}. $cm^2.mol^{-1}$) = 73.8, Zn% theoretical (practical) = 8.03 (7.96).

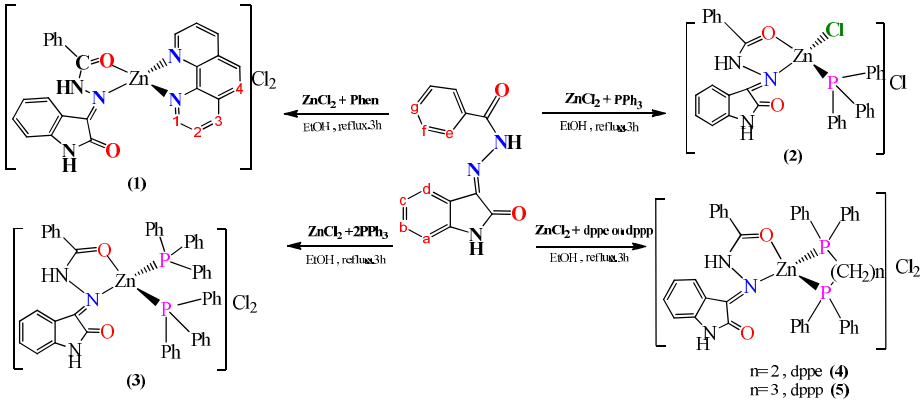

Scheme 2. Synthesis Zn(II) complexes (**1-5**).

Evaluation of the antibacterial activity of the synthesized Zn(II) complexes

The antibacterial (biological) activity of the synthesized complexes was evaluated against four types of bacteria - two Gram-positive (*Staphylococcus aureus* (ATCC 25923), and *Streptococcus faecalis* (ATCC 29212)) and two Gram-negative (*Pseudomonas aeruginosa* (ATCC 27853), and *Escherichia coli* (ATCC 25922)) using the agar well diffusion method [8, 21].

The procedure

The zinc complexes were prepared in DMSO at concentrations of (1×10^{-3}, 1×10^{-4}, and 1×10^{-5} M). For the culture medium, 38 g of nutrient agar was dissolved in 1 L of distilled water, heated until fully dissolved, then autoclaved at 121 °C and 15 bar for 15 min. After cooling, the medium was poured into Petri dishes to solidify.

To evaluate biological activity, 53.5 g of Mueller-Hinton agar was prepared similarly. After sterilization, bacterial samples were spread on the agar and incubated at 37 °C for 24 hours. Four 5 mm holes were made in the agar, and 1 mL of each zinc complex solution was added. The plates were incubated for another 24 hours. Amikacin at 10^{-5} M served as a reference, and inhibition zones were measured with a ruler for comparison.

Cytotoxicity and cell viability assay (MTT) [14]

The cytotoxicity of the prepared compounds $[Zn(L)(Phen)]Cl_2$, $[Zn(L)(PPh_3)_2]Cl_2$, $[Zn(L)(dppe)]Cl_2$, and $[Zn(L)(dppp)]Cl_2$ was tested against human liver cancer cell lines (Hep-G2) using the method described in the literature [22, 23]. Briefly, 2.9 × 103 cells were seeded in a 96-well plate and incubated for 24 hours, followed by the addition of different concentrations (5-500 μM) of the studied complexes for 48 hours, and compared with (Cis-platin) as a positive control. After the specified treatment period, MTT (3-[4,5-dimethylthiazol-2-yl]-2,5-diphenyl-2H- tetrazolium bromide) was added to each well, followed by incubation of the plate for another 3 hours before the addition of dimethyl sulfoxide (DMSO). Then, the absorbance of each well was measured using a Tecan M200 Infinite Pro-microplate Reader at 570 nm, with a reference wavelength of 650 nm. Absorbance is measured at a wavelength of 570 nm because it is the optimal wavelength for detecting the conversion of the MTT compound into formazan, which is the substance produced by the activity of living cells. When there is cellular activity and viability, the MTT compound is converted into formazan, which has a high absorbance at 570 nm. As for the 650 nm wavelength, it is used to compensate for any nonspecific effects, such as scattering in measurements or optical interferences. This helps improve the accuracy of the reading by removing unwanted signals that may affect the precision of calculating cell viability. The percentage of cell viability was calculated by reference to the untreated control, and the IC_{50} value was recorded by plotting the percentage of survival against the concentration of the test compound on a logarithmic scale using the Graph-Pad Prism 9 software.

RESULTS AND DISCUSSION

Molar conductivity measurement

The zinc complexes No. **1**, **3**, **4**, and **5** exhibited molar conductivity values in the range of (73.8-85.4) $ohm^{-1}.\ cm^2.\ mol^{-1}$, indicating the presence of two chloride (Cl^-) ions outside the coordination sphere. In contrast, the complex **2** $[Zn(L)(PPh_3)Cl]Cl$ showed a molar conductivity value in the range of 32.7 $ohm^{-1}.cm^2.mol^{-1}$, suggesting the presence of only one chloride (Cl^-) ion outside the coordination sphere [24]. These molar conductivity data are consistent with the proposed structural formulas for these zinc complexes, which are further supported by the other analyses and measurements carried out.

FTIR spectrum of the ligand and zinc complexes

The ligand was characterized by studying its infrared spectrum and comparing it with the FTIR spectra of the starting materials used in its preparation. A strong band appeared at 1695 cm^{-1}, which was attributed to the stretching vibration of the new (C=O) group of the ligand [24]. The

disappearance of the carbonyl (C=O) band of the free isatin, which usually appears around 1730 cm^{-1}, was observed. The appearance of a new strong band at 1620 cm^{-1} was assigned to the stretching vibration of the (-CH=N-) group [25, 26], indicating the formation of the ligand. The spectrum also showed a band at 1676 cm^{-1}, corresponding to the stretching vibration of the (C=O) group at position 1 of the ligand. Additionally, a band at 3199 cm^{-1} was observed, which was assigned to the N-H stretching vibration [22], and a band at 3089 cm^{-1} was present, corresponding to the aromatic (C-H) stretching vibration. The FTIR spectral analysis provided evidence for the successful synthesis and formation of the ligand [23, 24], as shown in Figure 1.

The infrared spectrum of the ligand (L) and its zinc complexes, as shown in Figure 1, demonstrates that the stretching vibration of the carbonyl (C=O) group which is located at position 2 and azomethine (-CH=N-) group are shifted to a lower frequency in which confirms that the oxygen and nitrogen atoms are coordinated with zinc ion. Additionally, the spectra of the zinc complexes **1**, **3**, **4**, and **5** showed weak bands around the range (550 cm^{-1}), (490 cm^{-1}) which are attributed to (M-O), and (M-N) groups, respectively [23, 26, 27], and complex **2** showed strong band at (390 cm^{-1}) assigned to (M-Cl) group [28]. Furthermore the spectra of the complexes (**4** and **5**) also exhibited a new band at the position (1422 and 1433 cm^{-1}), respectively, which was assigned to the vibrational frequency of the phenyl groups bonded to the phosphorus ν(Ph-P) and two bands were observed at (1099, 690 cm^{-1}) assigned to the ν(C-P) group [27]. Additively, the spectra displayed a band at (2920 cm^{-1}) corresponding to the ν(C-H) aliphatic stretching vibration of the phosphine [23].

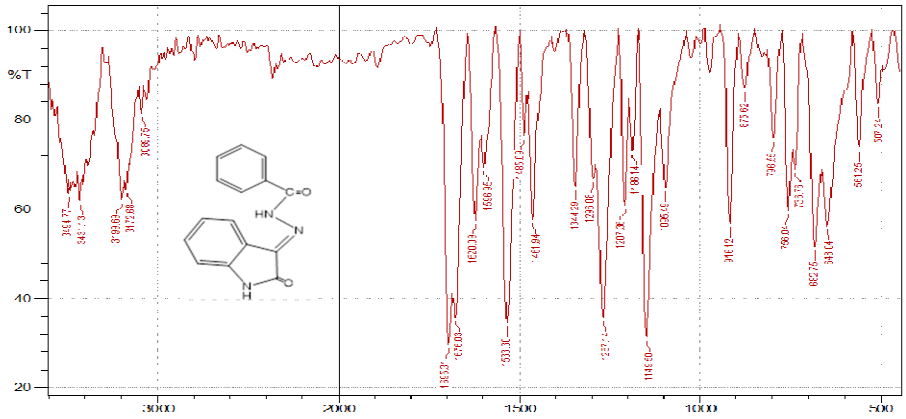

Figure 1. FTIR spectrum of the ligand (L).

^{1}H, $^{13}C\{^{1}H\}$, and $^{31}P\{^{1}H\}$–NMR spectra data

^{1}H-NMR spectrum of the ligand showed a singlet signal at the chemical shift (δ = 13.93 ppm), corresponding to the amidic (NH) group. The spectrum also showed a singlet signal at the chemical shift (δ =11.37 ppm), corresponding to the (NH) group in the isatin moiety. Furthermore, the spectrum exhibited a doublet signal at the chemical shift (δ = 7.88 ppm) with coupling constant of ($^{3}J_{H-H}$ = 7.70 Hz), which was assigned to the H_e and a triplet signal at the chemical shift (δ=7.60ppm) with coupling constant of ($^{3}J_{H-H}$ = 7.62 Hz), which was assigned to the H_f protons. Additionally, the spectrum displayed a doublet signal at the chemical shift (δ = 7.67 ppm) with coupling constant of ($^{3}J_{H-H}$ = 7.59 Hz), attributed to the H_a proton. The spectrum also showed a triplet signal at the chemical shift (δ = 7.38 ppm) with coupling constant of ($^{3}J_{H-H}$ = 7.13 Hz), which was assigned to the H_c proton.

Furthermore, the spectrum exhibited a triplet signal at the chemical shift (δ =7.10 ppm) with a coupling constant of ($^3J_{H-H}$ = 7.68 Hz), assigned to the H_b proton. Furthermore, the spectrum displayed a doublet signal at the chemical shift (δ = 6.95 ppm) with an integration of one proton and a coupling constant of ($^3J_{H-H}$ = 7.88 Hz), attributed to the H_d proton [24, 28].

While the ^{1}H–NMR spectra for the all zinc complexes (**1-5**) showed a singlet signal at the chemical shift (δ = 13.94-13.97 ppm), assigned to the amide (NH) group. The spectrum also showed a singlet signal at the chemical shift (δ = 11.37-11.48 ppm) assigned to the (NH) group in the isatin moiety. Additionally, the complexes **4** and **5** were showed a triplet signal at (δ = 2.73 ppm) corresponding to the terminal ($2CH_2$) groups. Furthermore, the triplet and multiple signals were observed at (δ = 2.73 and 1.73 ppm), attributed to the central (CH_2) group of the dppp ligand in the complex [29, 30], as illustrated in the Figures in the supplementary file.

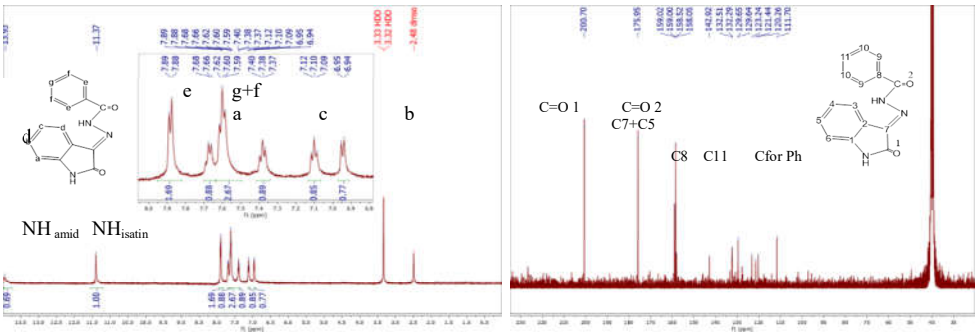

Figure 2. ^{1}H and ^{13}C{^{1}H}-NMR of the ligand.

The ^{13}C{^{1}H}-NMR spectrum of the ligand showed a signal at (δ = 200.70 ppm) which was attributed to the carbon of the (C=O) group within the ring. Additionally, the spectrum displayed a signal at (δ = 175.95 ppm) which was assigned to the carbon of the (C=O) group. Furthermore, the spectrum exhibited four signals within the range of (δ = 158.05-159.02 ppm) which were attributed to C7, C1, C8, and C11 respectively. Additionally, a signal at (δ = 142.92 ppm) was assigned to C5.The remaining carbon signals appeared in the range of (C = 111.70-132.51 ppm) [7, 30], as shown in the Figure 2.

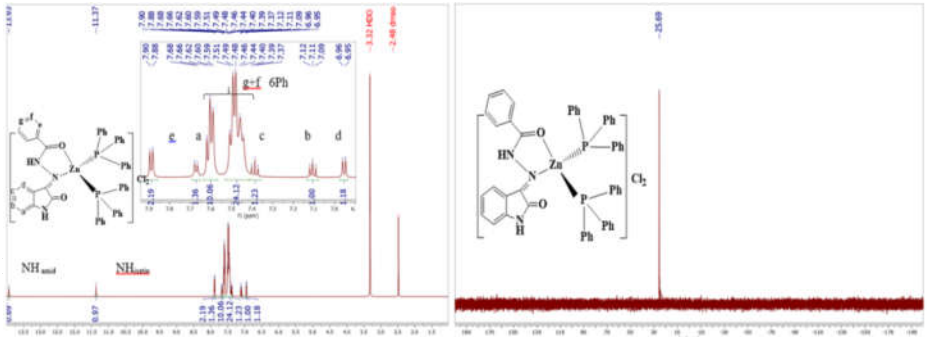

Figure 3. ^{1}H{^{31}P}and ^{3}1P{1H}-NMR spectrum of the complex **3**.

$^{31}P\{^{1}H\}$-NMR spectrum study for the complex **2** $[Zn(L)(PPh_3)_2Cl]Cl$, showed the broad signal at δ_P = 32.61 ppm which suggests the presence of a single isomer of the complex **2** $[Zn(L)(PPh_3)Cl]Cl$. The disappearance of the other signals upon cooling the sample solution indicates that there are dynamic processes occurring in the complex, which is slowed down at lower temperatures, leading to the simplification of the spectrum [26, 29].

The $^{31}P\{^{1}H\}$-NMR spectrum of the complex **3** $[Zn(L)(PPh_3)_2]Cl_2$ showed a prominent singlet signal at the chemical shift (δ_P = 25.69 ppm), which indicates the presence of a single isomer and the equivalence of the two phosphorus atoms in the tetrahedral complex[26, 29], as shown in Figure 3.

The $^{31}P\{^{1}H\}$-NMR spectra of the complexes **4**, and **5** $[Zn(L)(dppe)]Cl_2$,and $[Zn(L)(dppp)]Cl_2$, showed a major singlet signal at the chemical shift δp = 29.97 , 57.70 ppm, respectively, indicating the equivalence of the two phosphorus atoms in the two complexes, which suggest that the dppe, and dppp ligands behave as a bidentate chelating ligand in the complexes [28, 30].

Thermogravimetric analysis (TGA)

The thermogravimetric curve can provide information related to the thermal stability, reaction kinetics, chemical composition of the sample, as well as the thermal stability of the products. TGA allows for the evaluation of the thermal stability of the complexes by monitoring the mass changes that occur as the temperature is increased. The data obtained from the TGA analysis can provide insights into the decomposition mechanisms, phase transitions, and the presence of volatile components in the samples. The data presented in Table 1 show results that are consistent with the proposed general formula of the complexes. The table also provides information for each stage of the weight loss during the (TG) analysis of the complex, where: T_i = the temperature at which the decomposition in a single step begins. T_f = the temperature at which the decomposition in a single step ends. T_{max} = the temperature of maximum weight loss.

Table 1. Thermogravimetric analysis (TGA) data for the prepared complexes **1**, **3**, and **5**.

Complexes	Step	T_i/°C	T_f/°C	T_{DTG} max	Weight mass loss %		Reaction	Total mass loss%
					Calc.	Found		
$[Zn(L)(Phen)]Cl_2$	1	241.04	319.18	258.46	27.07	27.13	$C_{12}H_{10}N_2O$	67.90
	2	319.18	654.85	370.18	36.21	36.25	$C_{12}H_6Cl_2N_2O$	67.66
	3	654.85	805.81	712.13	4.38	4.50	CH_6N	
							3C + ZnO	
The percentage of the practical weight loss %67.90, and the residue %32.10. The percentage of the theoretical weight loss %67.66, and the residue %32.34.								
$[Zn(L)(PPh_3)]Cl_2$	1	198.41	279.22	246.54	16.95	17.00	$C_9H_{15}N_2O$	83.61
	2	279.22	340.49	298.56	36.61	36.73	$C_{17}H_{10}Cl_2NP_2$	86.82
	3	340.49	804.92	398.78	33.45	33.88	$C_{19}H_{13}$	
							ZnO	
The percentage of the practical weight loss %87.61, and the residue %12.39.The percentage of the theoretical weight loss %86.82, and the residue %13.18.								
$[Zn(L)(dppp)]Cl_2$	1	60.77	270.34	232.67	16.98	17.00	$C_9H_8N_2O$	75.78
	2	270.34	402.65	329.97	36.39	39.73	$C_{20}H_{22}ClNP_2$	75.97
	3	403.65	804.75	455.19	33.88	33.45	$C_{12}H_9Cl$	
							C + ZnO	
The percentage of the practical weight loss %57.78, and the residue %24.22. The percentage of the theoretical weight loss %75.97, and the residue %24.03.								

This information from the TG analysis can provide insights into the thermal stability and decomposition behavior of the prepared complexes. The thermogravimetric (TG) analysis of the complex $[Zn(L)(Phen)]Cl_2$ shows that it decomposes in three stages. The diagram depicts the mechanism of the weight loss stages for the complex and the critical temperature at which the maximum transformation of the compound (maximum weight loss) occurs. The experimental and theoretical percentages of weight lost at each stage are indicated in the mechanism. The results in Table 2 show that the experimental weight loss is 67.88% and the remaining weight is 32.12%, while the theoretical weight loss is 67.66% and the remaining weight is 32.34%. The remaining material is identified as the metal oxide (ZnO +3C). This detailed TG analysis provides insights into the thermal decomposition behavior and the composition of the final residue for the $[Zn(L)(Phen)]Cl_2$ complex [31].

Results of bacterial sensitivity to some prepared compounds

After conducting the tests related to the efficiency of the solutions towards different bacterial genera, diverse results were obtained among the prepared compounds. Two types of Gram-negative bacteria and two different types of Gram-positive bacteria were selected, all of which are considered pathogenic to humans and animals. The results showed that some solutions had antimicrobial activity against the selected bacterial genera, despite the resistance of some of them to antibiotics. As for the other solutions that did not show antimicrobial activity against the selected bacterial genera, as shown in Table 2.

Table 2. The inhibitory activity of prepared zinc(II) complexes on four types of (G+) and (G–) bacteria (inhibition zone diameter measured in mm).

Complexes	Concentration	*Pseudomonas aeruginosa* G–	*Escherichia coli* G–	*Staphylococcus aureus* G+	*Streptococcus faecalis* G+
$[Zn(L)(phen)]Cl_2$	10^{-3}	19	20	21	19
	10^{-4}	0	12	15	13
	10^{-5}	0	2	6	8
$[Zn(L)(PPh_3)_2]Cl_2$	10^{-3}	16	19	22	20
	10^{-4}	0	15	12	12
	10^{-5}	0	0	0	6
$[Zn(L)(PPh_3)Cl]Cl$	10^{-3}	0	20	0	6
	10^{-4}	0	15	0	2
	10^{-5}	0	0	2	2
$[Zn(L)(dppe)]Cl_2$	10^{-3}	17	2	12	0
	10^{-4}	12	2	0	0
	10^{-5}	0	0	0	0
$[Zn(L)(dppp)]Cl_2$	10^{-3}	17	16	20	8
	10^{-4}	10	9	12	8
	10^{-5}	0	0	0	6

The microbial inhibition zones of the solutions ranged between 9 to 22 mm, except for the solutions that did not show any effect on the bacteria, indicating that these solutions have diverse biological activities depending on the concentrations used. The complexes $[Zn(L)(Phen)]Cl_2$ and $[Zn(L)(dppp)]Cl_2$ showed the highest inhibition at the lowest concentration against (*Streptococcus faecalis*). From the antibacterial data of these complexes, we observed that their sensitivity or resistance is influenced by the lipophilic nature of the metal ion, which can change through chelation with free ligands. This affects the permeability of the bacterial membrane, either allowing or preventing the complexes from passing through the lipoid layer of the bacteria. Furthermore, the stereochemistry of these ligands (Phen), and (dppp) is crucial for their antimicrobial activity, potentially enhancing their binding with the amino acids of (*Streptococcus*

faecalis). Other factors such as solubility, conductivity, electron density, molecular size, membrane permeability, and concentration also impact the activity of the synthesized complexes. As for the Gram-negative bacteria, the complex $[Zn(L)(Phen)]Cl_2$ gave the highest inhibition rate at the lowest concentration, reaching (2 mm), which is a weak effect, while the other complexes did not give any significant effect on (*Escherichia coli*). The studied complexes did not affect the species (*Pseudomonas aeruginosa*) at the lowest inhibitory concentration [26, 28].

Anticancer activity of the prepared compounds

The anticancer activities of the studied complexes were tested against human liver cancer cell lines (Hep-G2) using the 3-(4,5-dimethylthiazol-2-yl)-2,5-diphenyl tetrazolium bromide (MTT) assay [32, 33]. The required concentrations of the prepared compounds for 50% inhibition concentration (IC_{50}) and cell viability percentage (%) are listed in Tables 3 and 4, as well as Figure 4. The results are compared with cisplatin as a standard anticancer drug. The complexes $[Zn(L)(Phen)]Cl_2$, and $[Zn(L)(dppe)]Cl_2$ showed in Table 4 have the highest inhibitory effect, with an IC_{50} value of 31.12 ± 1.57 μM and57.24 ± 1.79 μM, respectively. While the complexes $[Zn(L)(dppp)]Cl_2$ and $[Zn(L)\ (PPh_3)_2]Cl_2$ have higher IC_{50} values of 65.16 ± 1.87 μM and 113.8 ± 2.15 μM, respectively, indicating lower cytotoxicity compared to the first two complexes. These results suggest that the $[Zn(L)(Phen)]Cl_2$ complex has the most potent anti-cancer activity against the (Hep-G2) liver cancer cell line among the tested compounds. The increased activity of the complex $[Zn(L)(Phen)]Cl_2$ can be attributed to the presence of a nitrogen atom in the heterocyclic ring, which can potentially form hydrogen bonds with DNA bases. Furthermore, the planar structure of Phen enables it to coordinate more effectively than phosphine ligands, which face steric hindrance from the phenyl groups bonded to the phosphorus atoms [34]. The $[Zn(L)(dppe)]Cl_2$ complex also demonstrates promising cytotoxicity, while the $[Zn(L)(dppp)]Cl_2$ and $[Zn(L)(PPh_3)_2]Cl_2$ complexes exhibit lower inhibitory effects. The differences in the IC_{50} values reflect the relative potency of the zinc(II) complexes and could be attributed to factors such as the nature of the ligands (Phen, PPh_3, dppp, dppe) and their influence on the overall structure and reactivity of the complexes [18].

Table 3. The cell viability (%) of the prepared compounds against the (Hep-G2) cell line.

Concentration (μM)	Cell viability (%)*			
	$[Zn(L)(Phen)]Cl_2$	$[Zn(L)(PPh_3)_2]Cl$	$[Zn(L)(dppe)]Cl_2$	$[Zn(L)(dppp)]Cl_2$
0.000	100.0	100.0	100.0	100.0
5	95.4	94.7	93.5	95.4
10	58.6	86.7	71.4	70.4
25	25.6	59.9	51.0	51.2
50	24.3	46.6	37.3	38.1
250	14.3	32.3	25.8	14.9
500	12.8	31.9	22.4	12.8

* These values are average for triplicate times.

Table 4. The IC_{50} values of the synthesized zinc compounds against the (Hep-G2) cell line in comparison to *cis*-platin.

Compound	IC_{50} value (μM)
NAS 73 = $[Zn(L)(Phen)]Cl_2$	31.12 ± 1.57
NAS 74 = $[Zn(L)(PPh_3)_2]Cl_2$	113.8 ± 2.14
NAS 88 = $[Zn(L)(dppp)]Cl_2$	57.24 ± 1.79
NAS 89 = $[Zn(L)(dppe)]Cl_2$	65.16 ± 1.87
Cis-platin	1.98 ± 0.11

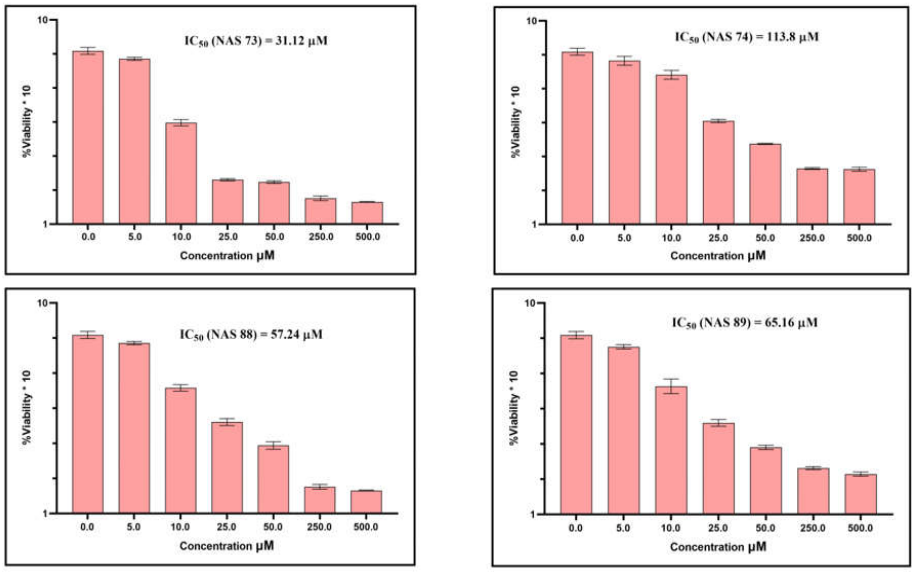

Figure 4. The anticancer activity of Zn(II) complexes against (Hep-G2) cell lines at different concentrations (μM). The p-value = 0.005 in each case.

CONCLUSION

Five zinc(II) complexes were prepared using the ligand *N′*-(2-oxoindolin-3-ylidene) benzohydrazide (L) and co-ligands such as Phen, dppp, dppe, and PPh_3. The ligand L coordinates in a bidentate chelating manner through oxygen and nitrogen atoms, while the co-ligands also coordinate in a bidentate fashion. We made two complexes with PPh_3 in 1:1 and 2:1 ratios, where PPh_3 functions as a monodentate ligand. Some of the complexes exhibited good thermal stability, decomposing in multiple stages. The antibacterial activity was evaluated, showing the $[Zn(L)(Phen)]Cl_2$ and $[Zn(L)(dppp)]Cl_2$ complexes had the highest inhibition against *Streptococcus faecalis* at the minimum concentration tested. For Gram-negative bacteria, the $[Zn(L)(Phen)]Cl_2$ complex exhibited the highest inhibition at a concentration of 10^{-3} M, while it showed the lowest inhibition at 10^{-5} M, indicating a weak effect at that lower concentration. The cytotoxicity of the $[Zn(L)(Phen)]Cl_2$, $[Zn(L)(PPh_3)_2]Cl_2$, $[Zn(L)(dppp)]Cl_2$, and $[Zn(L)(dppe)]Cl_2$ complexes was tested against human liver (Hep-G2) cell lines. The $[Zn(L)(Phen)]Cl_2$ complex exhibited the highest inhibitory effect, with an IC_{50} of 31.12 ± 1.57 micromolar, compared to the other studied complexes.

ACKNOWLEDGEMENTS

The authors gratefully acknowledge the support and use of facilities provided by the University of Sulaimani, College of Science, Department of Chemistry during the course of conducting this research. The authors would also like to express their sincere appreciation to the University of Tikrit, College of Education of Pure Science, Department of Chemistry for their support and for providing access to their laboratory facilities for the practical work carried out as part of this study.

REFERENCES

1. Maugard, T.; Enaud, E.; Choisy, P.; Legoy, M.D. Identification of an indigo precursor from leaves of *Isatis tinctoria* (Woad). *Phytochemistry* **2001**, 58, 897-904.
2. Pandeya, S.N.; Smitha, S.; Jyoti, M.; Sridhar, S.K. Biological activities of isatin and its derivatives. *Acta Pharm.* **2005**, 55, 27-46.
3. Pakravan, P.; Kashanian, S.; Khodaei, M.M.; Harding, F.J. Biochemical and pharmacological characterization of isatin and its derivatives: from structure to activity. *Pharmacol. Rep.* **2013**, 65, 313-335.
4. Batanero, B.; Barba, F. Electrosynthesis of tryptanthrin. *Tetrahedron Lett.* **2006**, 47, 8201-8203
5. Doménech, A.; Doménech-Carbó, M.T.; Del Río, M.S.; De Agredos Pascual, M.L.V.; Lima, E. Maya Blue as a nanostructured polyfunctional hybrid organic–inorganic material: The need to change paradigms. *New J. Chem.* **2009**, 33, 2371-2379.
6. Dehaghani, M.Z.; Yousefi, F.; Seidi, F.; Bagheri, B.; Mashhadzadeh, A.H.; Naderi, G.; Esmaeili, A.; Abida, O.; Habibzadeh, S.; Saeb, M.R.; Rybachuk, M. Encapsulation of an anticancer drug isatin inside a host nano-vehicle SWCNT: A molecular dynamics simulation. *Sci. Rep.* **2021**, 11, 18753.
7. Walker, S.J.; Archer, P.; Banks, J.G. Growth of *Listeria monocytogenes* at refrigeration temperatures. *J. Appl. Bacteriol.* **1990**, 68, 157-162.
8. Kriza, A.; Parnau, C. Complexes of tin(IV) with some bidentate Schiff bases derived from 1ihiindoli-2,3idione. *Acta Chim. Slov.* **2001**, 48, 445-452.
9. Kakkar, R. Isatin and its derivatives: A survey of recent syntheses, reactions, and applications. *Med. Chem. Comm.* **2019**, 10, 351-368.
10. Sridhar, S.K.; Saravanan, M.; Ramesh, A. Synthesis and antibacterial screening of hydrazones, Schiff and Mannich bases of isatin derivatives. *Eur. J. Med. Chem.* **2001**, 36, 615-625.
11. Gao, N.; Kramer, L.; Rahmani, M.; Dent, P.; Grant, S. The three-substituted indolinone cyclin-dependent kinase 2 inhibitor 3-[1-(3H-Imidazol-4-yl)-meth-(Z)-ylidene]-5-methoxy-1,3-dihydro-indol-2-one (SU9516) kills human leukemia cells via down-regulation of mcl-1 through a transcriptional mechanism. *Mol. Pharmacol.* **2006**, 70, 645-655.
12. Li, H.H.; Zhang, X.H.; Tan, J.Z.; Chen, L.L.; Liu, H.; Luo, X.M.; Shen, X.; Lin, L.P.; Chen, K.X.; Ding, J.; Jiang, H.L. Design, synthesis, antitumor evaluations and molecular modeling studies of novel 3, 5-substituted indolin-2-one derivatives. *Acta Pharmacol. Sin.* **2007**, 28, 140-152.
13. Bal, T.R.; Anand, B.; Yogeeswari, P.; Sriram, D. Synthesis and evaluation of anti-HIV activity of isatin β-thiosemicarbazone derivatives. *Bioorg. Med. Chem. Lett.* **2005**, 15, 4451-4455.
14. Aziz, N.M.; Abdullah, B.H. Synthesis, cytotoxicity, antibacterial activity and molecular modeling study of new mono, homo and heterobimetallic complexes of palladium(II) with some transition metal ions containing the ligands N-phenyl-N'-(2-thiazolyl) thiourea and diphosphines $Ph_2P(CH_2)_nPPh_2$ (where n = 1–3). *Indian J. Chem. A* **2019**, 58, 772-782.
15. Al-Mudhafar, M.M.J.; Omar, T.N.; Abdulhadi, S.L. Bis-Schiff bases of isatin derivatives synthesis, and their biological activities: A review. *Al Mustansiriyah J. Pharm. Sci.* **2022**, 22, 23-48.

16. Goel, A.; Aggarwal, N.; Jain, S. Novel methodology for synthesis and computational analysis of zinc complexes of isatin derivatives and screening their biological activity. *Anti-Infective Agents* **2022**. 20, 46-55.
17. Alshdoukhi, I.F.; Al-barwari, A.S.; Aziz, N.M.; Khalil, T.; Faihan, A.S.; Al-Jibori, S.A.; Al-Janabi, A.S. Pd(II), Pt(II), Zn(II), Cd(II) and Hg(II) complexes of the newly prepared 1,2-benzo-isothiazol-3 (2H)-dithiocarbamate (BIT-DTC) ligand. *Bull. Chem. Soc. Ethiop.* **2024**, 38, 889-899.
18. Aziz, N. Palladium(II) mixed ligand complexes of benzoisothiazol-3 (2H)-dithiocarbamate (bit-dtc) and tertiary diphosphines: Synthesis, characterization, biological and anticancer studies. *Baghdad Sci. J.* **2024**, DOI: 10.21123/bsj.2024.9491.
19. Abbas, N.; Khan, I.; Batool, S.; Ali, M.; Farooq, U.; Khan, A.; Hameed, S.; White, J.M.; Ibrar, A. 2-Nitrobenzohydrazide as a potent urease inhibitor: synthesis, characterization and single crystal X-ray diffraction analysis. *J. Chem. Soc. Pak.* **2018**, 40, 1.
20. da Silva, G.A.; de Castro, A.C.; Mendes, R.K.S.; das Neves Moreira, D.; da Silva Cavalcanti, G.R.; da Fonseca, M.G.; João Pedro Agra Gomes, J.P.A.; de Alencar-Filho, E. B.; Vaz, B.G.; dos Santos, G.F.; Gesiane da Silva Lima, G.; da Silva, F.F.; Lima-Junior, C.G. Bentonite catalyzed solvent-free synthesis of N′-(2-oxoindolin-3-ylidene) benzohydrazide derivatives under microwave irradiation. *J. Mol. Struct.* **2022**, 1270, 133914.
21. Mohammed, B.A.K.; Ahmed, S.A.; Al-Healy, F. Design, characterizations, DFT, molecular docking and antibacterial studies of some complexes derived from 4-aminpantipyrine with glycine amino acid and ligand. *Bull. Chem. Soc. Ethiop.***2024**, 38, 1609-1624.
22. Li, L.; Zhang, Y.Z.; Liu, E.; Yang, C.; Golen, J.A.; Rheingold, A.L.; Zhang, G. Synthesis and structural characterization of zinc(II) and cobalt(II) complexes based on multidentate hydrazone ligands. *J. Mol. Struct*. **2016**, 1110, 180-184.
23. Mohammed, L.W.; Irzoqi, A.A. New 3-hydrazonoindolin-2-one Cd(II) complexes with amino pyridine ligands, synthesis, characterization and biological activity evaluation. *Tikrit J. Pure Sci.* **2020**, 25, 38-46.
24. Akouibaa, M.; Kadiri, M.; Driouch, M.; Tanji, K.; Ouarsal, R.; Rakib, S.; Sfaira, M.; Morley, N.; Lachkar, M.; El Bali, B. ; Zarrouk, A.; Bendeif, E.E. Synthesis, catalytic activity, magnetic study and anticorrosive activity of mild steel in HCl 1 M medium of $(H_3dien)[Cu(NO_3)(C_2O_4)_2].2H_2O$. A redetermination at 100 K. *Mater. Chem. Phys.* **2023**, 307, 128130.
25. Thota, S.; Nadipelly, K.; Shenkesi, A.; Yerra, R.; Salhin, A.; Fun, H.K. Design, synthesis, characterization, antioxidant and in vitro cytotoxic activities of novel coumarin thiazole derivatives. *Med. Chem. Res.* **2015**, 24, 1162-1169.
26. Jirjes, H.M.; Irzoqi, A.A.; Al-Doori, L.A.; Alheety, M.A.; Singh, P.K. Nano cadmium(II)-benzyl benzothiazol-2-ylcarbamodithioate complexes: Synthesis, characterization, anti-cancer and antibacterial studies. *Inorg. Chem. Commun*. **2022**, 135, 109110.
27. Abouzayed, F.I.; Farahat, A.M.; Emara, E.M.; Abou El-Enein, S.A. Spectral, thermal, and biological activity studies of some nano divalent (E,Z)-methyl N {[(methylamino) carbonyl] oxy} ethanimidothioate metal chelates. *Results Chem.* **2023**, 6, 101184.
28. Al-Jibori, S.A.; Irzoqi, A.A.; Al-Janabi, A.S.; Al-Nassiry, A.I.; Basak-Modi, S.; Ghosh, S.; Wagner, C; Hogarth, G. Synthesis, structure and reactivity with phosphines of Hg(II) ortho-cyano-aminothiophenolate complexes formed via C–S bond cleavage and dehydrogenation of 2-aminobenzothiazoles. *Dalton Trans*. **2022**, 51, 7889-7898.
29. Irzoqi, A.A.; Salman, F.A.; Alasadi, Y.K.; Alheety, M.A. Synthesis and structural characterization of palladium(II) mixed-ligand complexes of N-(benzothiazol-2-yl) benzamide and 1,2-bis (diphenylphosphino) ethane. *Inorg. Chem*. **2021**, 60, 18854-18858.
30. Salih, M.M.; Irzoqi, A.A.; Alasadi, Y.K.; Mensoor, M.K. Synthesis, characterization and antibacterial activity of some Hg(II) complexes with mixed benzyl 2-(2-oxoindolin-3-ylidene)

hydrazinecarbodithioate and phosphines or amines ligands. *Trop. J. Nat. Prod. Res. (TJNPR).* **2021**, 5, 895-901.
31. Morgan, S.M.; Diab, M.A.; El-Sonbati, A.Z. Synthesis, molecular geometry, spectroscopic studies and thermal properties of Co(II) complexes. *Appl. Organomet. Chem.* **2018**, 32, e4305.
32. Haribabu, J.; Jeyalakshmi, K.; Arun, Y.; Bhuvanesh, N.S.; Perumal, P.T.; Karvembu, R. Synthesis, DNA/protein binding, molecular docking, DNA cleavage and in vitro anticancer activity of nickel(II) bis (thiosemicarbazone) complexes. *RSC Adv.* **2015**, 5, 46031-46049.
33. Anastasiadou, D.; Psomas, G.; Kalogiannis, S.; Geromichalos, G.; Hatzidimitriou, A.G.; Aslanidis, P. Bi-and trinuclear copper(I) compounds of 2,2,5,5-tetramethyl-imidazolidine-4-thione and 1,2-bis (diphenylphosphano) ethane: Synthesis, crystal structures, in vitro and in silico study of antibacterial activity and interaction with DNA and albumins. *J. Inorg. Biochem*. **2019**, 198, 110750.
34. Al-Doori L.A., Irzoqi A.A., Jirjes H.M., AL-Obaidi A.H., Alheety M.A. Zn(II)-isatin-3-thiosemicarbazone complexes with phosphines or diamines for hydrogen storage and anticancer studies. *Inorg. Chem. Commun.* **2022**, 140, 109454.